tvst

Article

Assessment of Choroidal Neovascularization Perfusion: A Pilot Study With Laser Speckle Flowgraphy

Giacomo Calzetti[1], Paolo Mora[1], Stefania Favilla[2], Giorgia Ottonelli[1], Giulia Devincenzi[1], Arturo Carta[1], Salvatore Tedesco[1], Anna Mursch-Edlmayr[3], Gerhard Garhöfer[4], Stefano Gandolfi[1], and Leopold Schmetterer[4,5,6,7,8,9]

[1] Ophthalmology Unit, University Hospital of Parma, Parma, Italy
[2] Independent Researcher, Parma, Italy
[3] Department of Ophthalmology, Kepler University Clinic, Johannes Kepler University, Linz, Austria
[4] Department of Clinical Pharmacology, Medical University of Vienna, Vienna, Austria
[5] Singapore Eye Research Institute, Singapore
[6] Nanyang Technological University, Singapore
[7] Ophthalmology and Visual Sciences Academic Clinical Program, Duke-NUS Medical School, Singapore
[8] Center for Medical Physics and Biomedical Engineering, Medical University of Vienna, Vienna, Austria
[9] Institute of Ophthalmology, Basel, Switzerland

Correspondence: Leopold Schmetterer, Singapore Eye Research Institute, 11 Third Hospital Avenue, 168751, Singapore. e-mail: leopold.schmetterer@seri.com.sg

Received: November 26, 2019
Accepted: March 3, 2020
Published: April 16, 2020

Keywords: laser speckle flowgraphy; imaging; choroid; age-related macular degeneration; anti-VEGF

Citation: Calzetti G, Mora P, Favilla S, Ottonelli G, Devincenzi G, Carta A, Tedesco S, Mursch-Edlmayr A, Garhöfer G, Gandolfi S, Schmetterer L. Assessment of choroidal neovascularization perfusion: a pilot study with laser speckle flowgraphy. Trans Vis Sci Tech. 2020;9(5):9, https://doi.org/10.1167/tvst.9.5.9

Purpose: The purpose of this study was to quantify perfusion in the area of choroidal neovascularization (CNV) using laser speckle flowgraphy (LSFG) before and after intravitreal anti-vascular endothelial growth factor (VEGF) injection.

Methods: Retrospective case series. Fifteen eyes of 15 patients with treatment-naïve CNV due to age-related macular degeneration (AMD) and with available LSFG images were included. The main outcome was the mean blur rate (MBR) quantified as a measure of perfusion within the CNV area observed on indocyanine green angiography. Twelve patients had available longitudinal data until one month after the injection, used to evaluate changes in perfusion, central macular thickness (CMT), visual acuity, and ocular perfusion pressure. Reproducibility of LSFG measurements was investigated at each time point from two images taken within five minutes.

Results: Intraclass correlation coefficients for LSFG measurements were higher than 0.8 indicating excellent reproducibility. There was a significant decrease in perfusion after one week (-26.4 $\pm$ 14.4%; $P = 0.027$), whereas, after one month, perfusion was no longer significantly different from baseline ($P = 0.121$). CMT showed a progressive decrease over the follow-up period. Changes in perfusion were strongly correlated with changes in CMT after one week, but not thereafter.

Conclusions: This pilot study suggests a method to select a region in the CNV area to quantify perfusion using LSFG. MBR could represent a parameter possibly related to regrowth of the CNV after anti-VEGF treatment. Large-scale studies are needed to assess the usefulness of LSFG in defining re-treatment criteria for neovascular AMD.

Translational Relevance: LSFG technology to quantify perfusion could provide useful biomarkers for therapeutic management of CNV.

Introduction

Age-related macular degeneration (AMD) is a leading cause of irreversible blindness in older adults worldwide.[1] The hallmark of the neovascular form of AMD (nAMD) is choroidal neovascularization (CNV), which is characterized by the abnormal growth of blood vessels originating from the choroid. The diagnosis of CNV currently relies on fluorescein angiography (FAG) and indocyanine green angiography (ICGA), which are time-consuming and invasive

techniques requiring dye injection that can cause adverse reactions. Moreover, extraction of quantitative blood flow data from these techniques has proven difficult.[2] Anti-vascular endothelial growth factor (VEGF) agents are the first-choice therapy for nAMD.[3,4] With these drugs, repeated administration is often required and the intervals between injections are commonly guided by optical coherence tomography (OCT). However, structural OCT cannot neither visualize the microvasculature nor can it quantify perfusion. In recent years, OCT angiography (OCTA) has been extensively used in nAMD[5–7] and it provided several signs of CNV changes before and after anti-VEGF.[8–11] However, quantitative measurement of perfusion with OCTA is challenging. Laser interferometry and laser Doppler flowmetry were also used for the assessment of CNV perfusion, but these techniques are not commonly used in clinical practice.[12–15]

Laser speckle flowgraphy (LSFG) is a promising technique for the exploration of ocular perfusion in a clinical setting given its patient friendliness and the real-time nature of measurement, however, its use in nAMD has received little attention so far.[16,17] To date, there is only one study on polypoidal choroidal vasculopathy (PCV),[18] a common sub-type of disease in Asian populations.[19] Another study included nine patients with different types of CNV but was published only as an abstract (Maekawa Y., et al. IOVS 2011;52:ARVO Abstract 6048). In the present pilot study, we propose a method for the quantification of perfusion in the area of CNV and we discuss its potential usefulness for the evaluation of intravitreal anti-VEGF therapy.

Materials and Methods

Patients

This pilot study was approved by the local ethics committee. Written informed consent was obtained and all procedures adhered to the tenets of the Declaration of Helsinki. Patients referred to the Ophthalmology Unit of the University Hospital of Parma (Italy) for nAMD have a baseline comprehensive evaluation including best corrected visual acuity (BCVA) assessment with the standard Early Treatment of Diabetic Retinopathy Study chart, dilated fundus examination, OCT (Cirrus HD-OCT 4000,Carl Zeiss Meditec, Dublin, CA, USA), FAG, and ICGA (Heidelberg Spectralis, Heidelberg Engineering, Heidelberg, Germany). In the patients included in this study, LSFG (RetFlow; Nidek Co. LTD, Gamagori, Aichi, Japan) was also performed a few hours before the first intravitreal injection, along with color fundus photography, BCVA, and OCT assessment. Patients with a diagnosis of treatment-naïve CNV type I, type II, or mixed type due to nAMD were included. Exclusion criteria were: diabetes mellitus, CNV type III, PCV, other ophthalmic diseases, such as glaucoma or other optic neuropathies, refractive error ≥6 diopters, significant opacities of the optical media (e.g. corneal scars, lens opacities classification system II grading ≥3, and posterior capsule opacification), and intraocular surgery within six months from baseline.

Table 1. Demographic and Baseline Clinical Characteristics of 15 Subjects Included in the Quantitative Analysis

Sex (M/F)	7/8
Age (years)	79.5 ± 7.6
Lens status (transparent lens/ cataract/pseudophakia)	4/6/5
CNV type (I/II/mixed)	7/0/8
Best-corrected visual acuity (logMAR)	0.63 ± 0.31
Central macular thickness (µm)	371.5 ± 87.2
Ocular perfusion pressure (mmHg)	57.5 ± 10.3

logMAR, logarithm of the minimum angle of resolution. Data are presented as means ± SD.

Fifteen eyes of 15 patients (7 men and 8 women; mean age, 79.5 ± 7.6 years; age range, 66–93 years) were quantitatively studied with LSFG at baseline (Table 1). Longitudinal data were available in 12 of these subjects at 1 week and at 1 month after the first intravitreal injection: 7 patients received bevacizumab 1.25 mg/0.05 mL, 4 received ranibizumab 0.5 mg/0.05 mL, and 1 received aflibercept 2 mg/0.05 mL. Clinical characteristics and study outcomes of these 12 subjects are reported in Table 2. Furthermore, we included one male patient (patient P16) aged 82 with treatment-naïve CNV, who was evaluated up to 1 month after completion of the loading phase (3 monthly injections of ranibizumab). Because this patient had no baseline ICGA because of prior allergic reactions, his LSFG images were analyzed qualitatively.

Laser Speckle Flowgraphy

In our study, we used a commercially available LSFG system (RetFlow; Nidek Co. LTD). The device consists of a fundus camera supplied with a 830-nm diode laser and a digital charge-coupled device camera (750 × 360 pixels). The spatial resolution is determined by the pixel size, which is 8.4 × 9.8 µm. The principles of the technology have been described in detail elsewhere.[16,20] Briefly, moving erythrocytes cause

Table 2. Clinical Characteristics and Study Outcomes of 12 Patients with Longitudinal Data

Sex (M/F)		5/7		
Age (years)		80.3 ± 6.7		
Lens status (transparent lens/ cataract/pseudophakia)		3/5/4		
CNV type (I/II/mixed)		4/0/8		
Parameter		**Baseline**	**1-week**	**1-month**
Mean blur rate, AU	mean ± SD	14.5 ± 5.4	10.4 ± 3.8	11.7 ± 4.3
	P value	Baseline vs. 1-week, 0.027	1-week vs. 1-month, 0.475	Baseline vs. 1-month, 0.121
BCVA, LogMAR	mean ± SD	0.68 ± 0.29	0.59 ± 0.25	0.64 ± 0.24
	P value	Baseline vs. 1-week, 0.407	1-week vs. 1-month, 0.677	Baseline vs. 1-month, 0.677
CMT, µm	mean ± SD	377.3 ± 90.6	326.2 ± 77.5	283.5 ± 45.7
	P value	Baseline vs. 1-week, 0.099	1-week vs. 1-month, 0.166	Baseline . 1-month, 0.004
OPP, mm Hg	mean ± SD	55.1 ± 10.2	55.2 ± 8.0	54.6 ± 9.6
	P value	Baseline vs. 1-week, 0.987	1-week vs. 1-month, 0.996	Baseline vs. 1-month, 0.990

a blurring of the speckle pattern, which is produced by the lights reflected from the ocular tissue. The output parameter is the mean blur rate (MBR), which represents a quantitative index of relative blood flow velocity in arbitrary units (AUs) and is calculated using first-order speckle statistics. The observation field of one image covers 6 × 3.8 mm (maximum diagonal field of 21°). One scan consists of a total of 118 images captured at a rate of 30 Hz resulting in total measurement time of approximately 4 seconds. The device is equipped with internal and external fixation targets and incorporates an eye-tracking system to adjust for eye movements and to ensure that the same location is scanned over time. The built-in analysis software mathematically averages all 118 acquired frames to produce a "composite map" wherein MBR is displayed in either a false color-scale image or a grayscale image.

LSFG Acquisition Protocol

Because one LSFG scan does not allow to cover the whole posterior pole, the acquisition was guided by ICGA and color fundus images. First, CNV extent was manually delineated on an early-to-mid-phase ICGA image using the "Draw function" of Spectralis (Heidelberg Engineering). Baseline CNV lesion size was also measured on this image using the area-measuring software provided by Spectralis, as described previously.[21,22] LSFG was then started and the live capture image was visually compared with the ICGA image to direct the scan toward the CNV by slowly moving the fixation target. Larger retinal and choroidal vessels visible on both images were used as visual benchmarks (see Fig. 1). Once the CNV was centered on the LSFG map, the scan was acquired. Scans that did not pass the automatic quality check were excluded and repeated until a good quality was achieved. This procedure was performed for the first scan, whereas the "follow-up function" of LSFG was used for follow-up measurements. This function allows to retrieve fixation position and laser intensity of a previously acquired scan. All LSFG images were acquired by one experienced operator under mydriatic conditions obtained with one drop of tropicamide 1%. Patients were asked to abstain from coffee, tea, and alcohol intake on the day of the LSFG examination, as these substances are known to potentially affect MBR.[23] Baseline and follow-up scans were recorded at the same time of the day (usually in the afternoon) in order to minimize the effects of diurnal variation.[24] Blood pressure and Goldmann applanation tonometry were measured shortly after LSFG, while subjects were comfortably sitting in a chair.

CNV Analysis

On the first LSFG image of each subject, an elliptical region of interest (ROI) was drawn within the CNV area. The selection of this elliptical region was based on

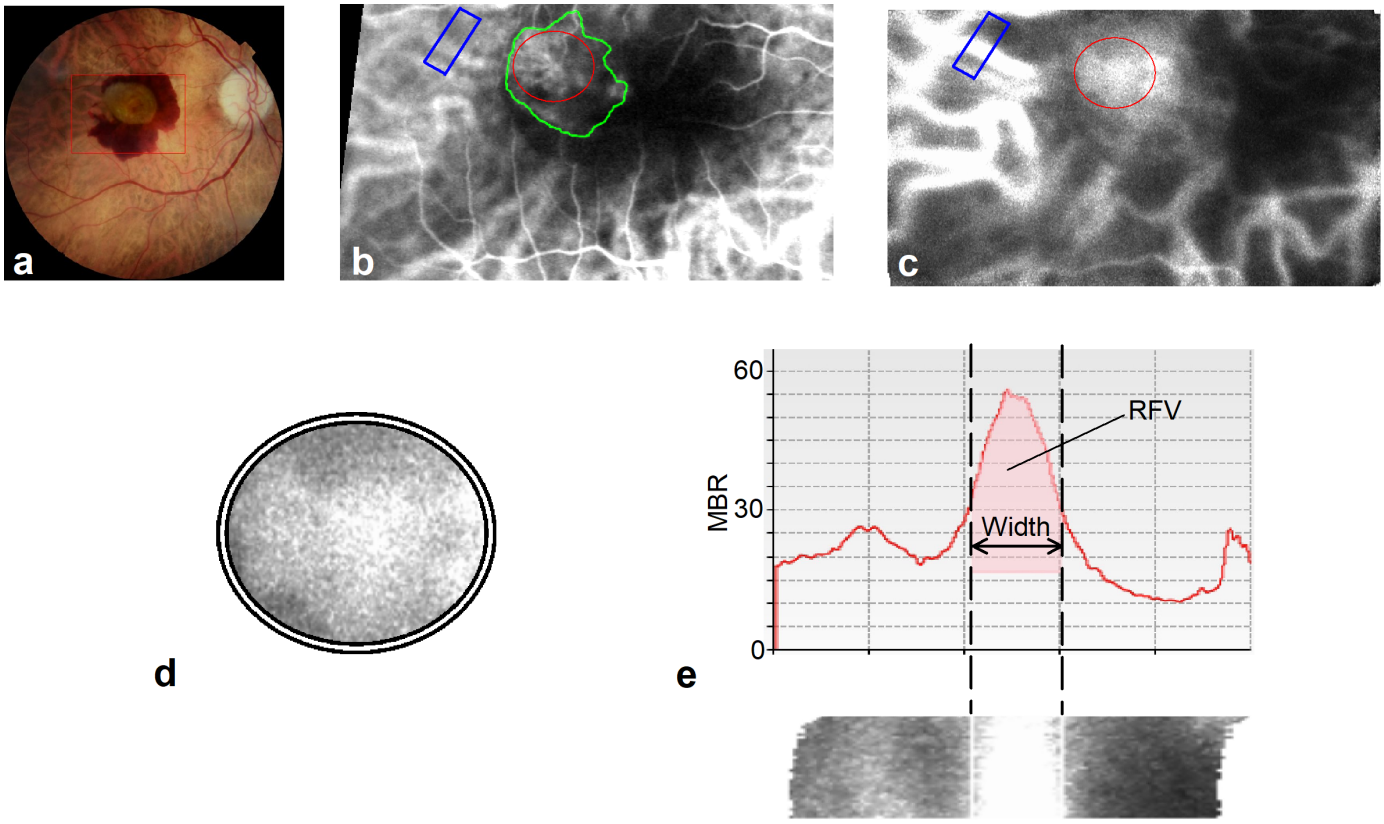

Figure 1. Multimodal imaging of a treatment-naïve choroidal neovascularization (CNV) in patient P1. (a) Color fundus photograph. The red rectangle identifies the region measured with the laser speckle flowgraphy (LSFG). (b) intermediate phase indocyanine green angiography (ICGA): the green region of interest (ROI) defines the CNV extent, which was manually drawn using the "Draw function" of Spectralis; the red elliptical ROI corresponds to the LSFG ROI, which was used to analyse perfusion in the CNV area. Note that the hemorrhage in a was not included in the LSFG ROI. The blue rectangular ROI corresponds to the LSFG ROI, which was used to analyse perfusion in the feeder vessel. (c) Grayscale LSFG composite map. Regions of higher blood flow are depicted in white, whereas regions of lower blood flow are depicted in black. The two ROI correspond to those shown in b. (d) Magnification of the ROI, which was used to analyse perfusion in the CNV area. (e) Magnification of the ROI, which was used to analyse perfusion in the feeder vessel. The software provides a blood flow value in arbitrary units, which is represented by the parameter "Relative flow volume" (RFV), and the vessel diameter in pixels, which is represented by the parameter "Width."

the manual delineation in the ICG image, as described above. Larger vessels visible on both images were used as visual benchmarks to perform this procedure. To avoid the masking effect, areas of hemorrhage and hard exudates detectable on color fundus photographs were not included in the ellipse. In addition, we took care not to include any visible larger retinal or choroidal vessels. In other words, the ROI in LSFG was the largest ellipse within the CNV area as observed in the ICGA, which did not include larger retinal or choroidal vessels, hemorrhage, and hard exudates. Therefore, the ROI in LSFG resulted smaller than the manually traced area in the ICGA image (Fig. 1). The MBR of all area within the ROI (defined as "Mean All" [MA]) was analyzed. All ROI positions and dimensions were saved and remained unchanged in the follow-up measurements.

Furthermore, feeder vessel blood flow was analyzed in one patient (patient P1) at all three time points. The feeder vessel was confirmed on ICGA and analyzed on the LSFG map using a rectangular ROI centered on the vessel, according to previously described methods (Fig. 1).[25] Briefly, the signal from this ROI contains information from the blood stream within the vessel as well as from the superimposed microvasculature. The signal from the larger vessel is automatically separated from MBR originating from the surrounding microvasculature by computing a threshold between MBR value. The on-board software finally extracts a blood flow value in AU defined as "relative flow volume" (RFV), and the vessel diameter as expressed in pixels. The formula for the calculation of RFV has been reported elsewhere.[26]

Central Macular Thickness Measurement

Central macular thickness (CMT) was assessed via the Central Subfield Thickness provided by the on-board analysis software of the Cirrus 4000 HD-OCT software version 7.0.2.5 (Carl Zeiss Meditec, Inc., Dublin, CA, USA). The measurement was centered on the fovea that was manually identified by an experienced operator on a "macular 512 × 128" scan.

Systemic Hemodynamics

Systolic blood pressure (SBP) and diastolic blood pressure (DBP) were measured using an automated oscillometric device (Dräger Infinity Delta; Dräger Inc., Telford, PA, USA). Mean arterial blood pressure (MAP) and ocular perfusion pressure (OPP) in the seated position were calculated as follows: MAP = DBP +1/3 (SBP–DBP), OPP = 2/3 MAP–IOP.

Statistical Analysis

Continuous variables were expressed as means ± SD. All the analyses were performed in R free software environment (R Core Team, 2017, http://www.R-project.org). Reproducibility analysis was carried out using two LSFG scans taken within five minutes by the same operator. The analysis was performed in 15 subjects prior to anti-VEGF treatment and in 12 subjects with longitudinal data at the post-treatment time points. Intraclass correlation coefficients (ICC; psych R package, https://CRAN.R-project.org/package=psych) were calculated to evaluate the reliability of MBR measurements at each time point. ICC of 0.75 and higher are considered as excellent reproducibility.[27] The study outcomes MBR, BCVA, CMT, and OPP were analysed with an ANOVA model for repeated measures in the 12 subjects with longitudinal data. For post hoc contrast analysis, a Fisher's Least Significant Difference test (95% family-wise confidence level) was applied. Furthermore, in order to quantify the associations between MBR and BCVA and between MBR and CMT, a repeated measures correlation coefficient (rmcorr R package https://CRAN.R-project.org/package=rmcorr) was estimated in the 12 subjects with longitudinal data. This algorithm allows to determine the common within-individual association for paired measures assessed on two or more time points for multiple individuals. Unlike simple regression/correlation, it does not violate the assumption of independence of observations and tends to have a greater statistical power because neither averaging nor aggregation is necessary for an intra-individual research question. The correlation analysis was tested considering the whole follow-up period and by paired intervals (i.e. baseline to 1 week, baseline to 1 month, and 1 week to 1 month). For all statistical analyses, a P value <0.05 was considered statistically significant.

Results

At baseline, OCT detected the presence of subretinal fluid (SRF) in 93% of cases (14/15 eyes) and intraretinal cystoid fluid (IRC) in 60% of cases (9/15 eyes). The mean CNV lesion size on ICGA was 2.66 ± 1.92 mm^2. The clinical characteristics of patients at baseline are summarized in Table 1. Complications arising from the intravitreal injection, such as endophthalmitis, vitreous hemorrhage, retinal pigment epithelium tear, or new macular hemorrhage did not occur in any of the patients included in the study. At 1 week, SRF and IRC were present in 83% (10/12 eyes) and 33% (4/12 eyes) of cases, respectively. At the 1 month time point, SRF was present in 50% (6/12 eyes) and IRC in 17% (2/12 eyes) of cases.

The mean size of the ROI, which was used to analyze perfusion in the CNV area, was 4892 ± 4204 pixels. ICC for MBR was 0.97 (95% confidence interval [CI], 0.91–0.99) at baseline, 0.98 (95% CI, 0.93–0.99) at the 1-week time point, and 0.97 (95% CI, 0.92–0.99) at the 1-month time point, respectively. There was a significant decrease of MBR at 1 week (1 week versus baseline, -26.4 ± 14.4%; $P = 0.027$), whereas after 1 month MBR was not significantly different from baseline any longer (1 month versus baseline, -17.7 ± 15.2%; $P = 0.121$). CMT showed a progressive decrease that reached statistical significance after 1 month compared to baseline ($P = 0.004$). The distribution of percent changes in CMT and MBR from baseline are shown in Supplementary Figs. 1 and 2. No significant changes were observed for BCVA and OPP (Table 2). Changes in MBR showed no significant correlation with changes in BCVA (whole follow-up period r = 0.168, $P = 0.422$; baseline to 1-week interval r = 0.306, $P = 0.310$; baseline to 1-month interval r = 0.126, $P = 0.681$; and 1-week to 1-month interval r = -0.245, $P = 0.419$). Changes in MBR significantly correlated with changes in CMT in the whole follow-up period (r = 0.511, $P = 0.009$), in the baseline to the 1-week interval (r = 0.642, $P = 0.018$) and in the baseline to 1-month interval (r = 0.652, $P = 0.016$), whereas there was no significant correlation in the 1-week to 1-month interval (r = -0.167, $P = 0.585$). Changes in MBR grouped by type of anti-VEGF agent are shown in Supplementary Fig. 3.

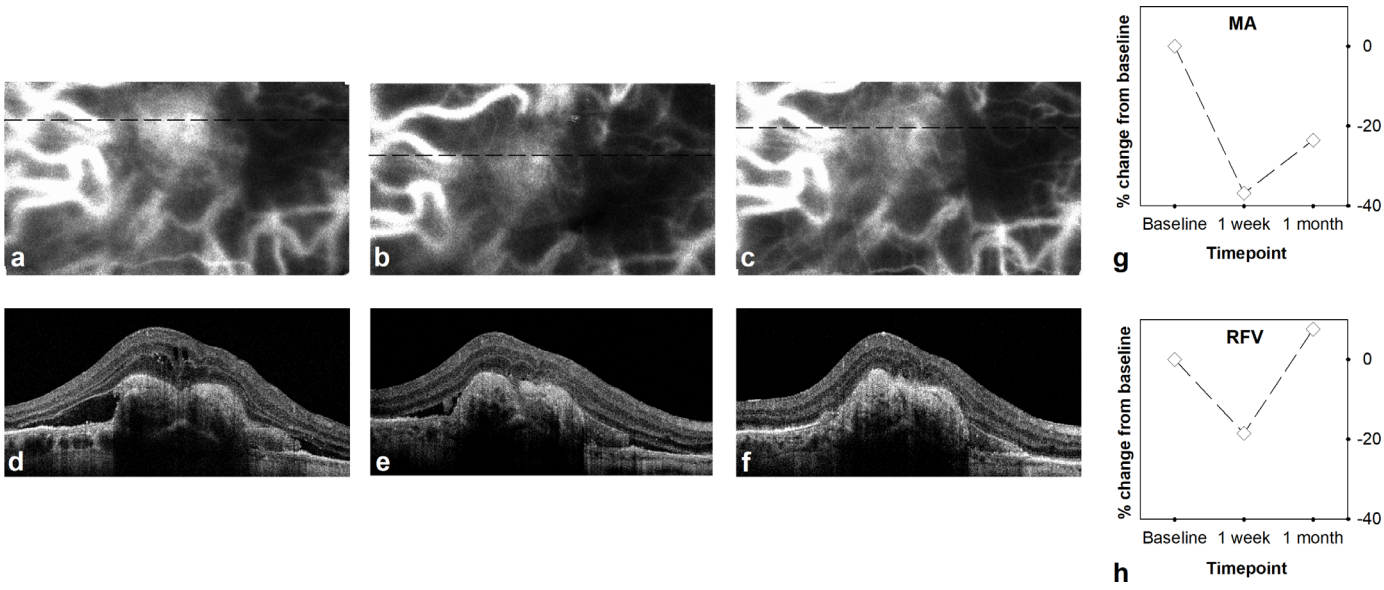

Figure 2. LSFG and OCT before and after intravitreal bevacizumab injection in patient P1. LSFG scans taken at baseline (a), one week (b), and one month (c) after bevacizumab intravitreal injection. Regions of higher blood flow are depicted in white, whereas regions of lower blood flow are depicted in black. The CNV area and the feeder vessel were analysed in the LSFG images using the regions of interest displayed in Figure 1. Horizontal black dashed lines indicate the position of the optical coherence tomography (OCT) B-scans shown in d to f. (d–f) OCT B-scans taken at baseline (d), one week (e), and one month (f) after bevacizumab intravitreal injection. Percent changes in mean blur rate (MBR) throughout the follow up in the area of CNV (g) and in the feeder vessel (h).

In patient P1, both MBR in the CNV area and RFV decreased from baseline to 1 week after injection. The decrease in MBR was almost twice the decrease in RFV. After 1 month, MBR was still approximately 20% lower than the baseline value, whereas RFV was 7% higher than the baseline value. OCT showed a progressive decrease in CMT and in fluid accumulation from baseline to 1 month after injection (Fig. 2).

Patient P16 had a CNV with an extensive type II component, which was evaluated up to 1 month after the third ranibizumab injection (Fig. 3). One week after the first injection, the LSFG map displayed a decrease in MBR in the CNV area, which was followed by an increase one month after the first and one month after the third intravitreal injection. Such an increase is more visible in larger vessels than in the microvasculature, indicating vascular remodeling.

Discussion

In our paper we propose an LSFG-based method to quantify perfusion in the CNV area identified by conventional dye-based angiography. In 12 patients affected by treatment-naive CNV, we collected longitudinal data before and after anti-VEGF intravitreal injection, quantifying early changes in perfusion and in clinical parameters occurring over one month. We observed a clear reduction in CNV perfusion at 1 week with partially recurrent blood flow at month one. To the best of our knowledge, no other technology is currently capable of obtaining quantitative perfusion parameters in response to anti-VEGF treatment.

Previously, LSFG was mainly used to assess perfusion at the optic nerve head in clinical studies. A drawback of this technology is the lack of depth resolution, which makes it difficult to isolate choroidal and retinal signal when an 830-nm wavelength is used, as in the commercially available LSFG system. However, Isono et al., after inducing branch retinal artery occlusion in the monkey macula, showed that 92% of the signal intensity of 830-nm LSFG originates from the choroid.[28] This proportion was in good agreement with the proportion between absolute choroidal and retinal blood flow rates in the monkey foveal region.[29] Subsequently, 830-nm LSFG was used to quantify macular choroidal perfusion in clinical studies of retinal disorders, such as PCV, acute central serous chorioretinopathy, retinitis pigmentosa, and diabetic retinopathy.[18,30–32] For the purpose of this study, we used a similar approach focusing on the macular area occupied by the CNV: the mean decrease in blood flow was 26% after 1 week. We recorded a pretty high variability of the response, which was, however, strongly correlated with CMT after one week. Variabil-

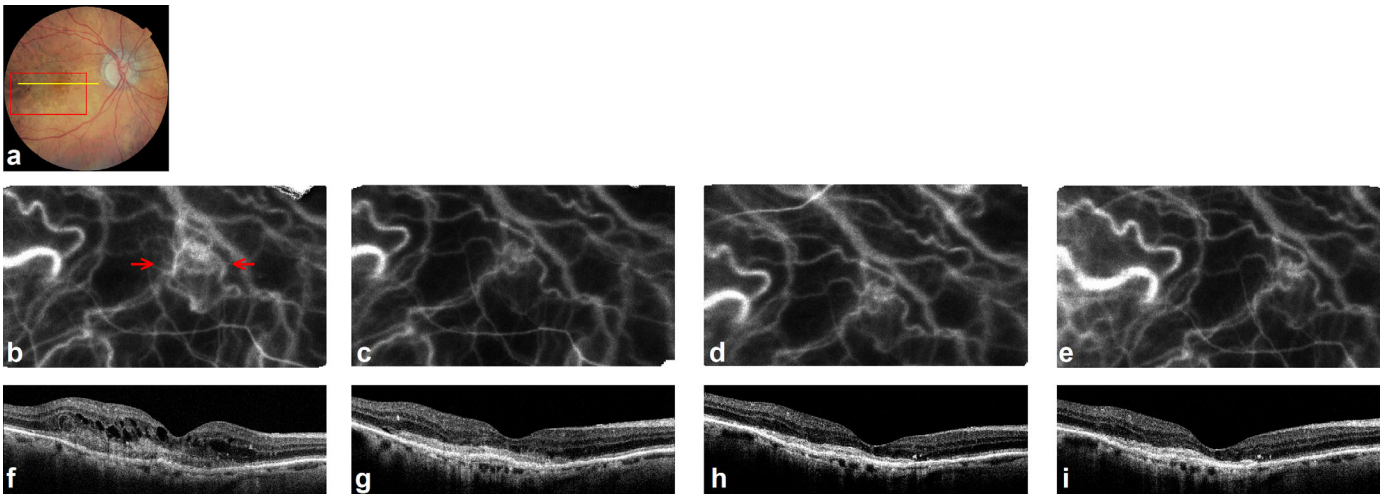

Figure 3. Multimodal imaging before and after intravitreal ranibizumab injection in patient P16. (a) baseline color fundus photograph. The red rectangle identifies the region measured with the LSFG, the yellow horizontal line indicates the position of the OCT B-scan shown in (f). (b–e) Grayscale LSFG perfusion maps taken at baseline (b), one week after the first injection (c), one month after the first injection (d), and one month after completion of the loading phase (3 monthly injections) (e). Regions of higher blood flow are depicted in white, whereas regions of lower blood flow are depicted in black. The CNV is indicated by the red arrows in (b). (f–i) Grayscale OCT scans taken at baseline (f), one week after the first injection (g), one month after the first injection (h), and one month after completion of the loading phase (i).

ity may be due to several factors, including patient responsiveness to anti-VEGF and type of anti-VEGF agent used. Interestingly, perfusion and CMT showed opposed trends thereafter. A very intriguing hypothesis is that the LSFG parameter may represent a parameter possibly related to regrowth of the CNV, but this needs to be proven in larger studies. Another option is that MBR increase was related to vascular remodeling within the CNV: pruning of small vessels with poor pericyte coverage would increase flow through the remaining larger vessels.[6] In this regard, a direct comparison with OCTA might provide useful details.

We cannot exclude that effects of anti-VEGF drugs on the retinal vasculature contributed to our results, but, as mentioned above, the contribution of retinal blood flow to the LSFG signal is considered to be small. Moreover, prior clinical studies in nAMD only reported a small effect of anti-VEGF agents on retinal blood flow. Using a bidirectional laser Doppler velocimeter, the mean decrease in retinal arteriolar blood flow was 1% and 6% one week and five weeks after bevacizumab injection, respectively.[33] It was also reported that retinal arteriolar diameter shows mild vasoconstriction after ranibizumab injection.[34] Additionally, the underyling choroid may potentially contribute to the LSFG signal obtained in our study. Previous studies using different technologies do, however, show a small effect of anti-VEGF drugs on choroidal circulation.[35–38] As such, the reduction in CNV perfusion after one week reported in the present study is unlikely to represent generalized choroidal vasconstriction.

Quantitative data on feeder vessel flow can be also extracted from the LSFG image if the vessel is clearly visible. For this kind of evaluation, feeder vessel blood flow was isolated after subtraction of the signal originating from the microvasculature surrounding the vessel. This method assumes that the surrounding microvasculature is comparable to the microvasculature superimposed on the feeder vessel. Validation of this approach for the measurement of perfusion in larger choroidal vessels was established by means of comparison with laser Doppler flowmetry in healthy subjects.[25] Measurement of feeder vessel perfusion might be of value in patients with nAMD, but again needs to be studied in a larger population.

Our study has some limitations related to the retrospective design and to the small sample size. Hence, it was impossible to compare our metrics under different treatment conditions and different anti-VEGF drugs. Furthermore, we acknowledge limitations intrinsic to the current LSFG system. These include: the limited field of observation, the use of relative units, and the lack of functional information, such as the leakage. Our approach may be not suitable in patients with a large amount of macular hemorrhage or lipid exudation. To avoid the masking effect of bleeding and lipid exudation, we actually measured within an area

that was smaller than that observed in ICGA and, as such, the measurement may not be representative of the whole CNV lesion. Retinal pigmentary changes occurring during the disease course should also be considered, although a method to correct MBR for fundus pigmentation is currently under development. Our approach has, however, the relevant advantage that it relies on commercially available equipment and can be easily implemented. Finally, we were unable to obtain choroidal thickness because of the limited penetration depth of our OCT device.

In conclusion, this pilot study describes an LSFG-based approach to extract data related to CNV quantitative perfusion. Prospective studies of longer duration are needed to assess the potential of MBR as biomarker for therapeutic management of nAMD.

Acknowledgments

The LSFG instrument was provided for free by Nidek. The company did, however, not influence data collection, evaluation or interpretation. The authors thank Pierangela Rubino for her critical help.

Disclosure: **G. Calzetti,** None; **P. Mora,** None; **S. Favilla,** None; **G. Ottonelli,** None; **G. Devincenzi,** None; **A. Carta,** None; **S. Tedesco,** None; **A. Mursch-Edlmayr,** None; **G. Garhöfer,** None; **S. Gandolfi,** None; **L. Schmetterer,** None

References

1. Lim LS, Mitchell P, Seddon JM, Holz FG, Wong TY. Age-related macular degeneration. *Lancet*. 2012;379:1728–1738.
2. van Stokkum IH, Lambrou GN, van den Berg TJ. Hemodynamic parameter estimation from ocular fluorescein angiograms. *Graefes Arch Clin Exp Ophthalmol*. 1995;233:123–130.
3. Rosenfeld PJ, Brown DM, Heier JS, et al. Ranibizumab for neovascular age-related macular degeneration. *N Engl J Med*. 2006;355:1419–1431.
4. CATT Research Group,Martin DF, Maguire MG,, et al. Ranibizumab and bevacizumab for neovascular age-related macular degeneration. *N Engl J Med*. 2011;364:1897–1908.
5. Jia Y, Bailey ST, Wilson DJ, et al. Quantitative optical coherence tomography angiography of choroidal neovascularization in age-related macular degeneration. *Ophthalmology*. 2014;121:1435–1434.
6. Spaide RF. Optical coherence tomography angiography signs of vascular abnormalization with antiangiogenic therapy for choroidal neovascularization. *Am J Ophthalmol*. 2015; 160:6–16.
7. Chua J, Tan B, Ang M, et al. Future clinical applicability of optical coherence tomography angiography. *Clin Exp Optom*. 2019;102:260–269.
8. Kuehlewein L, Sadda SR, Sarraf D. OCT angiography and sequential quantitative analysis of type 2 neovascularization after ranibizumab therapy. *Eye (Lond)*. 2015;29:932–935.
9. Huang D, Jia Y, Rispoli M, Tan O, Lumbroso B. Optical coherence tomography angiography of time course of choroidal neovascularization in response to anti-angiogenic treatment. *Retina*. 2015;35:2260–2264.
10. Coscas GJ, Lupidi M, Coscas F, et al. Optical coherence tomography angiography during follow-up: qualitative and quantitative analysis of mixed type I and II choroidal neovascularization after vascular endothelial growth factor trap therapy. *Ophthalmic Res*. 2015;54:57–63.
11. Mastropasqua L, Toto L, Borrelli E, Carpineto P, Di Antonio L, Mastropasqua R. Optical coherence tomography angiography assessment of vascular effects occurring after aflibercept intravitreal injections in treatment-naive patients with wet age-related macular degeneration. *Retina*. 2017;37:247–256.
12. Schmetterer L, Kruger A, Findl O, Breiteneder H, Eichler HG, Wolzt M. Topical fundus pulsation measurements in age-related macular degeneration. *Graefes Arch Clin Exp Ophthalmol*. 1998;236:160–163.
13. Metelitsina TI, Grunwald JE, DuPont JC, Ying GS, Brucker AJ, Dunaief JL. Foveolar choroidal circulation and choroidal neovascularization in age-related macular degeneration. *Invest Ophthalmol Vis Sci*. 2008;49:358–363.
14. Maar N, Pemp B, Kircher K, et al. Ocular haemodynamic changes after single treatment with photodynamic therapy assessed with non-invasive techniques. *Acta Ophthalmol*. 2009;87:631–637.
15. Boltz A, Luksch A, Wimpissinger B, et al. Choroidal blood flow and progression of age-related macular degeneration in the fellow eye in patients with unilateral choroidal neovascularization. *Invest Ophthalmol Vis Sci*. 2010;51:4220–4225.
16. Sugiyama T, Araie M, Riva CE, et al. Use of laser speckle flowgraphy in ocular blood flow research. *Acta Ophthalmol*. 2010;88:723–729.
17. Witkowska KJ, Bata AM, Calzetti G, et al. Optic nerve head and reti-

nal blood flow regulation during isometric exercise as assessed with laser speckle flowgraphy. *PLoS One*. 2017;12:e0184772.
18. Watanabe G, Fujii H, Kishi S. Imaging of choroidal hemodynamics in eyes with polypoidal choroidal vasculopathy using laser speckle phenomenon. *Jpn J Ophthalmol*. 2008;52:175–181.
19. Wong CW, Yanagi Y, Lee WK, et al. Age-related macular degeneration and polypoidal choroidal vasculopathy in Asians. *Prog Retin Eye Res*. 2016;53:107–139.
20. Sugiyama T. Basic technology and clinical applications of the updated model of laser speckle flowgraphy to ocular diseases. *Photonics*. 2014;1:220–234.
21. Costanzo E, Miere A, Querques G, Capuano V, Jung C, Souied EH. Type 1 choroidal neovascularization lesion size: indocyanine green angiography versus optical coherence tomography angiography. *Invest Ophthalmol Vis Sci*. 2016;57:OCT307–OCT313.
22. Told R, Sacu S, Hecht A, et al. Comparison of SD-optical coherence tomography angiography and indocyanine green angiography in type 1 and 2 neovascular age-related macular degeneration. *Invest Ophthalmol Vis Sci*. 2018;59:2393–2400.
23. Okuno T, Sugiyama T, Tominaga M, Kojima S, Ikeda T. Effects of caffeine on microcirculation of the human ocular fundus. *Jpn J Ophthalmol*. 2000;46:170–176.
24. Iwase T, Yamamoto K, Ra E, Murotani K, Matsui S, Terasaki H. Diurnal variations in blood flow at optic nerve head and choroid in healthy eyes: diurnal variations in blood flow. *Medicine (Baltimore)*. 2015;94:e519.
25. Calzetti G, Fondi K, Bata AM, et al. Assessment of choroidal blood flow using laser speckle flowgraphy. *Br J Ophthalmol*. 2018;102:1679–1683.
26. Shiga Y, Asano T, Kunikata H, et al. Relative flow volume, a novel blood flow index in the human retina derived from laser speckle flowgraphy. *Invest Ophthalmol Vis Sci*. 2014;55:3899–3904
27. Cicchetti DV. Guidelines, criteria, and rules of thumb for evaluating normed and standardized assessment instruments in psychology. *Psychol Assess*. 1994;6:284–290.
28. Isono H, Kishi S, Kimura Y, Hagiwara N, Konishi N, Fujii H. Observation of choroidal circulation using index of erythrocytic velocity. *Arch Ophthalmol*. 2003;121:225–231.
29. Alm A, Bill A. Ocular and optic nerve blood flow at normal and increased intraocular pressures in monkeys (Macaca irus): a study with radioactively labelled microspheres including flow determinations in brain and some other tissues. *Exp Eye Res*. 1973;15:15–29.
30. Saito M, Saito W, Hashimoto Y,, et al. Macular choroidal blood flow velocity decreases with regression of acute central serous chorioretinopathy. *Br J Ophthalmol*. 2013;97:775–780.
31. Murakami Y, Funatsu J, Nakatake S,, et al. Relations among foveal blood flow, retinal-choroidal structure, and visual function in retinitis pigmentosa. *Invest Ophthalmol Vis Sci*. 2018;59:1134–1143.
32. Mikoshiba Y, Iwase T, Ueno Y, Yamamoto K, Ra E, Terasaki H. A randomized clinical trial evaluating choroidal blood flow and morphology after conventional and pattern scan laser panretinal photocoagulation. *Sci Rep*. 2018;8:14128.
33. Fontaine O, Olivier S, Descovich D, Cordahi G, Vaucher E, Lesk MR. The effect of intravitreal injection of bevacizumab on retinal circulation in patients with neovascular macular degeneration. *Invest Ophthalmol Vis Sci*. 2011;52:7400–7405.
34. Papadopoulou DN, Mendrinos E, Mangioris G, Donati G, Pournaras CJ. Intravitreal ranibizumab may induce retinal arteriolar vasoconstriction in patients with neovascular age-related macular degeneration. *Ophthalmology*. 2009;116:1755–1761.
35. Rechtman E, Stalmans I, Glovinsky J,, et al. The effect of intravitreal bevacizumab (Avastin) on ocular pulse amplitude in neovascular age-related macular degeneration. *Clin Ophthalmol*. 2011;5:37–44.
36. Nitta F, Kunikata H, Aizawa N,, et al. The effect of intravitreal bevacizumab on ocular blood flow in diabetic retinopathy and branch retinal vein occlusion as measured by laser speckle flowgraphy. *Clin Ophthalmol*. 2014;8:1119–1127.
37. Okamoto M, Yamashita M, Ogata N. Effects of intravitreal injection of ranibizumab on choroidal structure and blood flow in eyes with diabetic macular edema. *Graefes Arch Clin Exp Ophthalmol*. 2018;256:885–892.
38. Mottet B, Aptel F, Geiser MH,, et al. Choroidal blood flow after the first intravitreal ranibizumab injection in neovascular age-related macular degeneration patients. *Acta Ophthalmol*. 2018;96:e783–e788.